RSC Advances

ROYAL SOCIETY OF CHEMISTRY

www.rsc.org/advances

Synthesis and characterization of UV-curable acrylate film modified by functional methacrylate terminated polysiloxane hybrid oligomer

HongleiWang[a,b,c], WeiquLiu[a,b*], ZhenlongYan[a,b,c], JianquanTan[a,b,c] and Guolun Xia-Hou[a,b,c]

[a] Guangzhou Institute of Chemistry, Chinese Academy of Sciences, Guangzhou 510650, China

[b] Key Laboratory of Cellulose and Lignocellulosics Chemistry, Chinese Academy of Sciences, Guangzhou 510650, China

[c] University of Chinese Academy of Sciences, Beijing 100049, China

* Corresponding author:

Email: liuwq@gic.ac.cn

Postal address: Prof. Weiqu Liu, Guangzhou Institute of Chemistry, Chinese Academy of Sciences, Guangzhou 510650, China

Tel: +86-20-85231660

Fax: +86-20-85231660

Abstract

A series of novel methacrylate terminated polysiloxane hybrid oligomer and functional acrylate oligomer were synthesized and characterized by GPC, FT-IR and NMR. Functional polysiloxane oligomer was introduced into acrylate UV-curing system to improve its surface and thermal properties. With increasing the content of organosiloxane segments, contact angle data of the UV-cured films increased, suggesting the organosiloxane segments migrated to the top surface. The SEM and EDS results demonstrated the migrating of organosiloxane segments. The refraction indexes results showed that the optical performance didn't reduce after organosiloxane segments being incorporated. According the TGA curves, the decomposition temperatures of the polysiloxane/acrylate composite UV-cured films were higher than that of pure acrylate UV-cured film, which demonstrated organosiloxane groups enhanced the thermal properties of acrylate film due to the high energy of the Si-C bond. The observation of the fractured-surface morphology showed that the organosiloxane segments floated onto the surface of the UV-cured films.

Keyword: Methacrylate terminated siloxane; Functional acrylate oligomer; UV-cured film; Hydrophobic surface

1. Introduction

UV-curing polymerization is widely used because of its beneficial properties [1-4], such as rapid curing speed, free-VOC, clean and efficient energy and moderate curing condition [5-8]. (Meth)acrylate groups have been employed widely for photopolymerization because of their strong reactivity, their characteristics of optical clarity, mechanical properties, adhesion and chemical stability, showing rapid, near-complete conversions (i.e., on residual unreacted monomers) with low heat generation [9]. Through the proper selection of acrylic/methacrylic monomers and curing agents, the cured polymers can be tailored to specific performance characteristics. Acrylic/methacrylic polymers form materials which are well known for their uses and applications in many important fields especially in the formulation of paints and surface coatings [10, 11]. However, in these applications materials with poor hydrophobicity are not useful unless they are modified. The acrylic/methacrylic polymers are inferior to some silicon-containing materials in terms of elasticity, flexibility, hydrophobicity and the heat resistance ability [12, 13]. In order to meet the need of high-performance coatings in high-technology areas, the UV-curable acrylic/methacrylic coating formulations must be continuously improved.

Polysiloxanes are the most important class of polymers with a non-carbon backbone, exhibiting a large degree of main-chain flexibility and high thermal stability due to Si-O groups [14-18]. Therefore, polysiloxanes have attracted much

interest and are widely used in modifying polyacrylate coatings. Nevertheless, there is a problem that polysiloxane isn't compatible well with polyacrylate due to their difference of solubility parameters. To solve this problem, many efforts have been made for the purpose of combining these two materials through chemical methods. Bourgeat-Lami, Bai and Zhao et al. researched on synthesis of polysiloxane and polyacrylate through emulsion polymerization [19-21]. Yu et al. synthesized and evaluated two series of polyacrylate-polydimethylsiloxane (PDMS) block and graft copolymers used in anti-icing coatings [22]. Mostly, research focused on incorporating polysiloxane into the main chain of a polymer, most frequently by emulsion polymerization methods, in order to improve the compatibility. However, emulsion polymerization products showed poor hydrophobicity. Thus, there is an ever increasing demand for polysiloxane modified polyacrylate with better defined, improved and novel physical, chemical and mechanical properties. In this research, we prepared polysiloxane oligomers and then introduced acrylic double bonds by the hydrolysis reaction with methacryloxy propyl trimethoxylsilane at a certain stage. Methacrylate terminated polysiloxane (MATSi) was thus obtained. Owing to the partly similar structure of methacryloxy propyl trimethoxylsilane and polyacrylate, the compatibility between functioned polysiloxane and polyacrylate could be improved.

The polyacrylate in this work was synthesized as a novel UV-curable polyacrylate (PA). 6-methylheptyl methacrylate was used as the major monomer since it could

provide good plasticity and was economic at the same time. Minor amount of hydroxyethylmethacrylate were added to promote adherence property. Glycidyl methacrylate was used to introduce epoxy groups to react with methacrylate (MA) in the following reaction step. Furthermore, a series of organosiloxane modified polyacrylate (OSPAs) at different organosilicone concentration ratios were respectively prepared by mixing PA with MATSi. In the presence of photoinitiator, OSPAs were crosslinked by the radical polymerization of the carbon-carbon double bonds in UV irradiation, and then the OSPA cured composite coatings were fast prepared. In this way, various properties and enhanced performance could be obtained in the form of OSPA cross-linked structure. The obtained polymers were characterized by gel permeation chromatography (GPC), fourier transform infrared (FT-IR) spectroscopy and nuclear magnetic resonance (NMR). Furthermore, the surface hydrophobic, optical, and thermal property of the cross-linked coatings made from obtained polymers was investigated by gel content test, flexibility test, pencil hardness test, contact angle (CA) analysis, refraction index test, scanning electron microscope, energy dispersive spectrometer, differential scanning calorimetry thermograms and thermogravimetric analyzer.

2. Experimental

2.1 Materials

Octaphenylpolyoxyethylene (OPE) was obtained from Quzhoumingfeng chemical company. Irgacure 1173 was obtained from Ciba Specialty Chemicals.

Dodecylbenzene sulfonic acid (DBSA), glycidyl methacrylate (GMA), hydroxyethylmethacrylate (HEMA), 6-methylheptyl methacrylate (MHMA), methacrylic acid (MA) and methacryloxy propyl trimethoxylsilane (KH570) were purchased from Aladding Industrial Corporation. Octamethylcyclotetrasiloxane (D_4) was provided by Guangzhou Jiahua chemical company. Distilled water, methanol, triethanolamine and azobisisobutyronitrile (AIBN) were purchased from Jingke Chemical Glass Instrument Co., Ltd. Butanone, tetrabutyl ammonium bromide (TBAB) and ethylalcohol were purchased from Sinopharm Chemical Reagent Co., Ltd. All the above materials were used as received without further purification.

2.2 Synthesis of polyacrylate

The polyacrylate was prepared by using 1:1:8 weight ratio of GMA, HEMA and MHMA in the presence of 4wt% AIBN as initiator and butanone as solvent at a temperature of 80^{o}C. The reaction was carried out in a four-neck reaction kettle equipped with mechanical stirring, nitrogen inlet, water condenser and thermometer. The reaction was carried out for 8 h to obtain desired product. Subsequently, butanone was removed by reduced pressure distillation. The retained desired product was labeled as GHM and was transported into another four-neck kettle. Afterwards, a certain amount of MA was added into the kettle in the presence of 0.8wt% TBAB. The reaction was carried out at 102^{o}C to reach 99.5% of the conversion determined by standard acid value. After remaining butanone and unreacted MA were discarded by reduced pressure distillation, the product was obtained and labeled as PA. The general

procedure was shown in Scheme 1.

Scheme 1.

2.3 Synthesis of MATSi

MATSi was synthesized by emulsion polymerization. The distilled water, surfactants (DBSA and OPE) and monomers (D_4) were added into a four-necked flask equipped with a thermometer, a reflux condenser, a mechanical stirrer and a nitrogen inlet. DBSA acted as acid catalyst as well. Nitrogen was added into the flask to remove oxygen at first. The reaction was carried out for 8 h at 80^{o}C with stirring at about 500rpm. After being neutralized with NaOH solution to stop the reaction, the final latex of PDMS was obtained. Then a certain quality of KH570 was added into PDMS latex. The condensation reaction of PDMS and KH570 was performed at 80^{o}C for 3 h. The copolymers were precipitated in ethanol and dried in vacuum drying oven. The product was purified in ethanol and hexane several times to remove the unreacted monomers and surfactants. Through this procedure, the product was obtained and designated as MATSi. The reaction scheme is shown in Scheme 2.

Scheme 2.

2.4 Preparation of OSPA UV curable films

PA and MATSi where used in relative mass ratios in the range of 100:0 to 90:10 as reported in Table 1. An amount of 5wt% photoinitiator (Irgacure 1173/triethanolamine = 2:3 w/w) was added into each formulation while stirring for 10 min. Triethanolamine was used to avoid the oxygen inhibition during the UV-curing process. Then films were cast onto a glass plate using 5% w/v solutions of the

copolymers in methanol by means of a wire-wound applicator. The coated films were laid in room temperature for at least 5 minutes until the solvent was evaporated. Then the films were irradiated by a high-pressure mercury lamp (500W) for 30s with a distance of 20 cm from lamp to the surface of samples in air atmosphere. The thickness of the final coating was about 100μm.

Table 1.

2.5 Characterization

The molecular weight and distributions of PA and MATSi oligomer samples were measured at 25^{o}C by gel permeation chromatography (GPC) on Waters 2410 instrument with THF as the solvent (1.0 ml/min) and polystyrene as the calibration standards.

The FT-IR spectra were recorded with TENSOR27, Bruker, Germany spectrometer over the range 400-4000cm^{-1}. ^{1}HNMR and ^{29}Si NMR were recorded with a 400MHz Bruker NMR spectrometer using $CDCl_3$ as solvent and tetramethylsilane as the internal reference.

The gel content method was performed on the cured films by measuring the weight loss after a 48-h extraction at 80^{o}C, according to the standard test method ASTM D2665-84[23]. Gel content was calculated as:

$$\text{Gel content} = \frac{Wt}{Wo} \times 100\% \qquad (1)$$

where W_0 is the initial weight of the film, and Wt is the final weight after extraction.

Flexibility of the UV-cured films was measured according to standard test method (ASTM D522) for elongation of attached coatings with conical mandrel apparatus (QTY-32, Shanghai Junda Co., China). Pencil hardness test was conducted on UV-cured films according to the Stander test method ASTM D2263.

The contact angle measurements were done by an optical contact angle meter (Shanghai Zhongchen, China) at room temperature (25^{o}C) using water and ethylene glycol as pendant drops. Each sample was tested more than 5 times at different locations and averaged readings were recorded to obtain a reliable value. The surface free energy was calculated by means of geometric–mean equation which was described by Owens and Wendt [24]. According to Owens and Wendt, the surface energy of a given solid can be determined using an equation applied to two liquids [24, 25].

$$(1+\cos\theta)\gamma_l=2(\gamma_s^{d}\gamma_l^{d})^{1/2}+2(\gamma_s^{nd}\gamma_l^{nd})^{1/2} \quad (2)$$

where γ_s and γ_l are the surface free energies of the solid and pure liquid, respectively. The superscripts ‘d’ and ‘nd’ represent the dispersive and non-dispersive contributions to the total surface energy, respectively. Water (γ_l=72.8mJ/m^2, γ_l^{d} =21.8 mJ/m^2, γ_l^{nd}=51 mJ/m^2), ethylene glycol (γ_l=48mJ/m^2, γ_l^{d}=29 mJ/m^2, γ_l^{nd} =19 mJ/m^2). According to Pinnau and Freeman[26], the contact angle, θ, in Eq. (2) was obtained from the following equation:

$$\theta= \cos^{-1}\left(\frac{\cos\theta_a+\cos\theta_r}{2}\right) \quad (3)$$

where θ_a and θ_r are the advancing and receding contact angles, respectively.

The refraction index of the coatings was determined by an Abbe refractometer (WAY-2W, Shanghai Electronics Physical Optics Instrument Co., Ltd) at 20^{o}C.

Scanning electron microscopy (SEM) and Energy dispersive spectrometer (EDS) were performed. Cross-section morphologies and elementary distribution of the fracture cured coating films were studied by environmental scanning electron microscopy (Hitachi S-4800 FESEM) with an energy dispersive spectrometer. For SEM inspection, samples were fixed to aluminum stubs with conductive tape prior to coating with ~20 nm of gold in an Ernest Fullam sputter coater.

The thermal stability of cured polymeric materials was determined using a thermogravimetric analyzer (TGA, TG209F3, NETZSCH, Germany). The thermogravimetric analysis of selected coatings were carried out at heating rate of 20^{o}C/min under nitrogen atmosphere (flow rate is 30 ml/min) in the temperature range of 40-600^{o}C. The differential scanning calorimetry (DSC) thermograms of UV-cured coating samples were performed using the DSC204 (NETZSCH, Germany) over the range from -60 to 120^{o}C at heating rate of 10^{o}C/min and held at 120^{o}C for 5 min to remove the thermal history under N_2 atmosphere.

3. Results and discussion

3.1 Synthesis and characterization of OSPA

Five UV-curable organosiloxane modified polyacrylates, OSPA1, OSPA2, OSPA3, OSPA4, OSPA5 were first prepared in this work in order to study the effects of silicon on the properties of UV-curable composite coatings. The general synthetic scheme for

the preparation of the copolymers used in the coating formulations is shown in Scheme 1 for PA and in Scheme 2 for MATSi. GPC, FT-IR, ^{1}HNMR and ^{29}SiNMR spectra were performed to measure the structures of the products. The molecular weights and polydispersity index of the oligomers were characterized by GPC. The typical molecular weight distributions for PA and MATSi were shown in Fig. 1. As shown in Table 2, the number-average molecular weight of PA and MATSi are 2740 and 1295 g/mol, respectively. The two mono-modal GPC curves suggested the formation of the two oligomers.

Fig. 1.

Table 2.

The recorded FT-IR spectra of GHM and PA were reported in Fig 2. Compared with the two traces of GHM and PA in Fig. 2, the disappearance of the characteristic absorption peaks of epoxide group at 910 cm^{-1} indicates the completion of the reaction. The peaks at 1640 cm^{-1} (methacrylate double bond) and 700 cm^{-1} (C-O-H bending) indicate that the epoxy groups have reacted by addition of MA by a ring-opening addition reaction producing one equivalent of hydroxyl groups. Simultaneously, C=C group was introduced into GHM. Absorbance at frequencies characteristic for acrylates (carbonyl C=O stretch at 1720cm^{-1}, C-O stretch four bands 1140cm^{-1} to 1180 cm^{-1}, 1180 cm^{-1} to 1280 cm^{-1},etc) are shown [27]. And meanwhile,

the characteristic absorption peaks at 1000 and 900 cm^{-1} for C-O is present in the spectra. Skeleton vibration of C=C group was also present at 483 cm^{-1}.

Fig. 2.

Fig. 3 shows the ^{1}HNMR spectra of PA in $CDCl_3$, peaks in the chemical shift range of 0.7-1.2 ppm and 1.3-1.7 ppm are assigned as $–CH_3$ (a, h, l, u, t) and $–CH_2$ (b, i, m, o, p, q, r), respectively. The protons resonance signals of –CH (s) and $–CH_3$ (g) appear in the region of 1.5-1.6 ppm and 1.7-2.0 ppm, respectively. The chemical shift of 3.6-3.7 ppm is attributed to protons of $HO–CH_2$ (k) and the chemical shift signals at 3.8-3.9 ppm are attributed to proton of HO-CH (d). The peaks at the chemical range of 4.0-4.2 ppm are corresponding to $O-CH_2$ (c, j, e, n). Peaks at 5.64-5.68 ppm and 6.11-6.18 ppm are assigned as the protons of $C=CH_2$ double bonds (f), indicating that epoxide groups reacted with methacrylic acid thus C=C photosensitive groups were introduced.

Fig. 3.

The ^{29}Si NMR signals of mono(T^1)-bi(T^2)-and tri(T^3)-fold Si-O-linked silicons can be typically observed in -45,…, -50 ppm, -55,…, -60 ppm and -65,…, -70 ppm region, respectively [28]. In Fig.4, the ^{29}Si NMR spectra of MATSi are shown. The signal at -68.8 ppm is usually assigned to T^3 which represents KH570 after condensation

polymerization. The signal of D^2 appears in the region of -21.8 ppm. It indicates the ring-opening and condensation polymerization reactions of Octamethylcyclotetrasiloxane. Poly(dimethylsiloxane) with hydroxyl group on the end is the product of the reactions. The peak at chemical shift of -19 ppm belongs to D^1 signal of Si-O group in MATSi structure. There are no signals in the region of -45,..., -50 ppm and -55,…, -60 ppm, which indicates there are no $T^1$and T^2 Si-O-linked silicons in the MATSi structure. It also manifests completely hydrolysis and condensation reactions of KH570. These results confirm that the MATSi is successfully prepared.

The FT-IR method was also used to confirm the reaction between ring-opened D_4 (PDMS) and KH570. From the IR spectra in Fig.5 it can clearly be observed that PDMS having characteristic peaks at 1018 cm^{-1} and 1089 cm^{-1} which are the characteristic absorption peaks of Si-O-Si. Si-CH_3 stretching vibration peak at 797 cm^{-1} was also observed. The peaks of Si-OH at 3699 cm^{-1} indicate that the ring in D_4 was opened and formed polysiloxane. The production MATSi was gained after PDMS reacting with KH570. The spectra of MATSi shows additional absorption peaks at 1722 cm^{-1}(C=O) and 1639 cm^{-1}(C=C) which represents the reaction between PDMS and KH570.

Fig. 4.

Fig. 5.

The five UV-cured formulations of PA and MATSi are similar to each other and OSPA3 was shown in Fig. 6. After irradiation, the characteristic C=C vibrations at 1640 cm^{-1} decreased apparently.

The characteristic peaks discussed above demonstrated the UV-curable hybrid oligomers based on acrylate containing organosilicone groups were successfully synthesized.

Fig. 6.

3.2 Degree of conversion in UV curing

FT-IR spectroscopy was used to determine the degree of conversion during the UV crosslinking reaction. The absorption band at 1640 cm^{-1} due to C=C vibration was monitored using FT-IR to determine the degree of conversion. The degree of conversion was determined using Eq. (4) [29, 30]

$$\text{Degree of conversion} = (1-\frac{At}{Ao})\times 100 \qquad (4)$$

where A_o is the absorption before UV exposure and A_t is the absorption after UV exposure. The coating formulation was coated on a KBr window and then exposed to UV radiation for 30 s. As shown in Fig. 7, the decrease in peak area of the C=C peak at 1640 cm^{-1} was monitored. Table 3 shows the degree of conversion in coatings after 30s of exposure to UV radiation. All of the OSPA formulations reached high conversion.

Fig. 7.

Table 3

3.3 Gel content, flexibility and hardness characterization of the UV-cured coatings

For the purpose of assessing the amount of insoluble part in cured films and the mechanical properties of the cured coatings, gel content measurements were conducted. In Table 4, the measured values are summarized. The gel content values of all the films are high enough to indicate the nearly complete cross-linked network of the pure PA and the composite OSPAs. In terms of flexibility, all of the composite OSPA samples passed the test of 8mm and 6mm diameter, and most of them passed the test of 5mm diameter, while the pure PA sample failed all the test of 8mm, 6mm and 5mm diameter. The hardness value of the samples rises from 3H to 6H with the increasing addition of MATSi. The flexibility and hardness test suggests that introduction of flexible silicon-oxygen segments enhanced mechanical properties of the UV-cured coatings.

Table 4.

3.4 Surface and optics characterization of the cured coatings

In order to determine the effect of organosilicone on surface and optical properties

of the UV-cured hybrid oligomers films, contact angle and refraction index were tested respectively. Table 5 presents the contact angle of the five samples. It can be seen that contact angle values of both water and ethylene glycol for pure PA film are much lower than any OSPA cured film. With the increasing of MATSi content, the contact angle values on OSPA cured film surfaces showed a gradually increasing change. It was found that based on the increase of organosilicone concentration, OSPA tended to be more hydrophobic compared with the virgin PA. Since organosilicone possesses low surface energy, they can easily move towards the air-polymer interface causing their enrichment on coating surface to some extent [31, 32]. Thereby, the presence of MATSi could lead to a great decrease in the surface free energy, and among these composite films, OSPA5 presented a very low surface free energy value down to 8.89 mN/m. Surfaces from mixtures of PA/ MATSi with a ratio of 1:0.02 still show hydrophobicity although the organosilicone content is low. The results shown in Table 5 indicate that organosilicone contribute to the surface hydrophobicity.

Table 5.

The refraction index of the coatings was measured by an Abbe refractometer at 20^{o}C. The obtained refraction indexes for samples OSPA1, OSPA2, OSPA3, OSPA4, and OSPA5 were listed in Fig. 8. As expected the refraction indexes ranged between 1.5612 and 1.5571 and are consistent with expected values for slight amount of

organosilicone content in the films. The refraction index of the samples gained a very small change with the increase of the organosilicone content which would not affect the optical properties of the composited material.

Fig. 8

3.5 Thermal properties of the cured coatings

Overall weight loss was observed in composite films with different organosilicone content. The TGA traces of all cured coatings are included in Fig.9, and plots of mass loss versus temperature are shown. To gain better understanding of the degradation behavior of the cured composite coatings, virgin PA film was compared with these composites at three specific degradation temperatures: (a) the temperature of the initial 5% mass loss ($T_{5\%}$); (b) the temperature of the 50% mass loss ($T_{50\%}$) and (c) residual weight percent at 600^{o}C. Three specific degradation data are summarized in Table 6. It shows that the typical onset temperature of the degradation is higher for the composites than the virgin PA. The thermal stability of the OSPA composites is enhanced relative to that of virgin PA. All the OSPA samples exhibit an apparent higher temperature at 50% weight loss during decomposition compared with pure PA. The different thermal properties between virgin PA and OSPA may be attributed to some interaction between organosilicone and PA that serves to stabilize the composite. The thermal stability of the composites systematically increases with increasing organosiloxane. The results demonstrate that the incorporated organosiloxane play an

important role during decomposition. The residual silicon-contained compound act as an insulator and mass transport barrier to the volatile products generated during decomposition. Meanwhile, compared with virgin PA, the more complex OSPA network reduced the overall rate of volatiles evolution.

Glass transition temperature (T_g) of the UV-cured films were investigated by differential scanning calorimetry (DSC). Fig. 10 shows the DSC thermograms of PA and OSPAs. The T_g value of all the samples are summarized in Table 6. There was an increasing trend of T_g value as the amount of MATSi in pure PA increasing.

Table 6. .

Fig. 9.

Fig. 10.

3.6 Micro-morphology of the cured coatings

Fig.11 shows the fractured-surface microstructure of the cured films cast onto glass slides from a PA/ MATSi ratio of 98:2, 96:4, 94:6, 92:8 and 90:10. Sample (a) exhibits a uniform distribution for the network of virgin PA. However, the fracture surface of OSPAs showed rougher features than that of virgin PA. These observations also indicate that the distribution of organosilicone copolymer in virgin PA is not homogeneous. In addition, it can be clearly observed that a certain extent of sphere

were enriched closed to the air side surface and there were also spheres in the matrix. This observation evidenced that the silicon-contained groups moved towards the air side surface of the cured films. These results can be explained as follows: During the solvent evaporation, silicon-contained groups move towards the top side surface of the UV-cured formulations owing to the poor compatibility with PA. These observations are in good agreement with the results obtained by contact angle value. When the content of MATSi increases, the phase separation appeared and became more obviously at the interphase [33-35]. It can be inferred that the hydrophobic surface may resulted from the silicon-contained segments in MATSi groups. The EDS results in Fig.12 showed energy-spectrum scanning from bottom to top of the film. It also indicated that the silicon-contained groups assembled on the surface of the films which agrees well with SEM and contact angle data. Furthermore, the silicon spheres are always at the end of the crack, which means they could efficiently absorb the energy generated in the fracture process and prevent aggravated fracture.

Fig. 11.

Fig. 12.

4. Conclusion

A novel methacrylate terminated polysiloxane was synthesized by hydrolysis reaction using octamethylcyclotetrasiloxane and methacryloxy propyl

trimethoxylsilane. Methacrylate groups were incorporated into functional polysiloxane oligomer to enhance the compatibility between organosiloxane segments and acrylate film. With the incorporation of organosiloxane OSPA gained increased thermal and mechanical properties compared to the virgin PA. Besides that, it was determined that owing to the hydrophobicity of organosilicone segments, the cured coating films containing PDMS had low surface free energy, and higher thermal degradation temperature. SEM and EDS studies of the coatings depicted that silicon-contained groups gathered on the air-side surface of the cured films. The low cost hydrophobic UV-curable OSPA coatings have a promising combination of physical and mechanical properties which will lead to potential application in industrial coatings fields such as printing inks, paints, adhesives and packaging overcoat film.

5. Acknowledgements

This study was financially supported by the Program “Tianhe District science and technology plan”.

References

[1] C. Chen, M. L. Li, Y. J. Gao, J. Nie and F. Sun, RSC Adv., 2015, 5, 33729.

[2] D. Knittel and E. Schollmeyer, Polym. Int., 1998, 45 (1): 110-117.

[3] K. J. van den Berg, L.G. J. van der Ven and H. J. W. van den Haak, Prog. Org. Coat., 2008, 61: 110-118.

[4] X. Liu, R. Liu, J. Zheng, Z. Li and J. liu, RSC Adv., 2015, DOI: 10.1039/C5RA03881B.

[5] S. P. Pappas, Radiation curing: science and technology, New York: Plenum, 1992.

[6] J. H. Lee, R. K. Prud'Homme, I. A. Aksay, J. Mater. Res., 2001, 16(12): 3536-3544.

[7] H. D. Hwang, C. H. Park, J. I. Moon, H. J. Kim and T. Masubuchi, Prog. Org. Coat., 2011, 72: 663-675.

[8] R. Mehnert, A. Pincus, I. Janorsky, R. Stowe and A. Berejka, UV and EB Curing Technology and Equipment, vol. I, SITA Technology Ltd., London, 1998.

[9] B. Türel Erbay and I. E. Serhatlı, Prog. Org. Coat., 2013, 76: 1-10.

[10] O. Chiantore, L. Trossarelli and M. Lazzari, Polymer, 2000, 41(5): 1657-1668.

[11] P. A. Christensen, A. Dilks, T. A. Egerton and J. Temperley, J. Mater. Sci., 1999, 34 (23): 5689-5700.

[12] S. J. Jeon, J. J. Lee, W. Kim, T. S. Chang and S. M. Koo, Thin Solid Films., 2008, 516: 3904-3909.

[13] H. Li, S. Liu, J. Zhao, D. Li and Y. Yuan, Thermochim. Acta., 2013, 573: 32-38.

[14] B. U. Ahn, S. K. Lee, S. K. Lee, J. H. Park and B. K. Kim, Prog. Org. Coat., 2008, 62: 258-264.

[15] H. D. Hwang and H. J. Kim, React. Funct. Polym., 2011, 71: 655-665.

[16] J. P. Lewicki, J. J. Liggat and M. Patel, Polym. Degrad. Stabil., 2009, 94: 1548-1557.

[17] S. W. Zhang, Z. D. Chen, M. Guo, J. Zhao and X. Y. Liu, RSC Adv., 2014, 4, 30938.

[18] M. Alexandre and P. Dubois, Mater. Sci. Eng: R: Reports., 2000, 28(1): 1-63.

[19] M. Lin, F. Chu, A. Guyot, J. L. Putaux and E. Bourgeat-Lami, Polymer., 2005, 46: 1331-1337.

[20] H. Li, S. Liu, J. Zhao, D. Li and Y. Yuan, Thermochim. Acta., 2013, 573: 32-38.

[21] R. Bai, T. Qiu, F. Han, L. He and X. Li, Appl. Surf. Sci., 2012, 258: 7683-7688.

[22] ASTM D2665-84, Standard Specification for Poly(Vinyl Chloride) (PVC) Plastic Drain, Waste, and Vent Pipe and Fittings, reapproved 2009.

[23] D. Yu, Y. Zhao, H. Li, H. Qi, B. Li and X. Yuan, Prog. Org. Coat., 2013, 76: 1435-1444.

[24] D. K. Owens and R. C. Wendt, J. Appl. Polym. Sci., 1969, 12: 1741-1747.

[25] T. Ç. Çanak and İ. E. Serhatlı, Prog. Org. Coat., 2013, 76: 388-399.

[26] Formation and modification of polymeric membranes: overview, in: I. Pinnau,B.D. Freeman (Eds.), 214th National Meeting of the American-Chemical-Society, Las Vegas, NE, 1997, pp. 1– 22.

[27] V. V. Krongauz, Thermochim. Acta., 2010, 503-504: 70-84.

[28] K. Albert, E. Bayer and B. Pfleiderer, J. Chrom., 1990, 506: 343.

[29] W. Xiao and W. Tu, J. Chem. Eng. Chin. Univ., 2009, 2: 13.

[30] I. Rehman, E. H. Andrews and R. Smith, J. Mater. Sci: Mater. Med., 1996, 7(1): 17-20.

[31] H. Tavana, F. Simon, K. Grundke, D. Y. Kwok, M. L Hair and A. W. Neumann,

J. Colloid. Interf. Sci., 2005, 291(2): 497-506.

[32] Y. S. Kim, J. S. Lee, Q. Ji and J. E. McGrath, Polymer., 2000, 43(25): 7161-7170.

[33] Z. Yan, W. Liu, N. Gao, H. Wang and K. Su, Appl. Surf. Sci., 2013, 284: 683-691.

[34] M. Sangermano, W. Carbonaro, R. Bongiovanni, R. R. Thomas and C. M. Kausch, Macromol. Mater. Eng., 2010, 295(5): 469-475.

[35] W. Liu, S. Ma, Z. Wang, C. Hu and C. Tang, Macromol. Res., 2010, 18(9): 853-861.

Figure captions:

Scheme 1. Synthesis route of UV-cured PA

Scheme 2. Synthesis route of MATSi

Figure 1. GPC traces of PA (a) and MATSi (b)

Figure 2. FT-IR spectra of GHM and PA

Figure 3. ^{1}H NMR spectra of PA

Figure 4. ^{29}Si NMR spectra of the synthesis of MATSi

Figure 5 FT-IR spectra of the synthesis of MATSi

Figure 6. FT-IR spectra of the synthesis of OSPA

Figure 7. FT-IR spectra of the UV-curable film formulations of PA and OSPAs. a) Before irradiation; b) After UV-curing

Figure 8. Refraction Indexes of the UV-cured coatings

Figure 9. TGA curves of the UV-cured coatings.

Figure 10. DSC thermograms of the UV-cured PA and OSPA coatings

Figure 11. SEM images of fractured-surface morphologies of the UV-cured coatings: (a)PA; (b)OSPA1; (c)OSPA2; (d)OSPA3; (e)OSPA4; (f)OSPA5.

Figure 12. EDS images of fractured surface of the UV-cured coatings

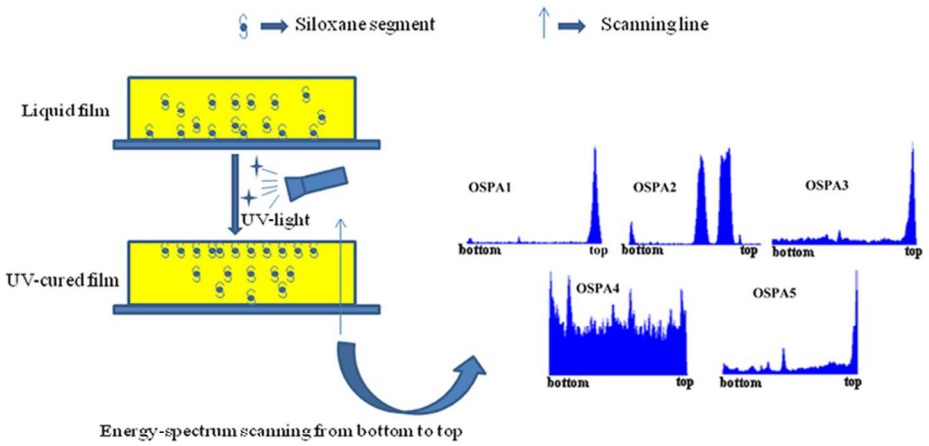

Graphical Abstract: Methacrylate terminated polysiloxane segments migrated to the top surface of the composite UV-curable polyacrylate film.
40x30mm (600 x 600 DPI)

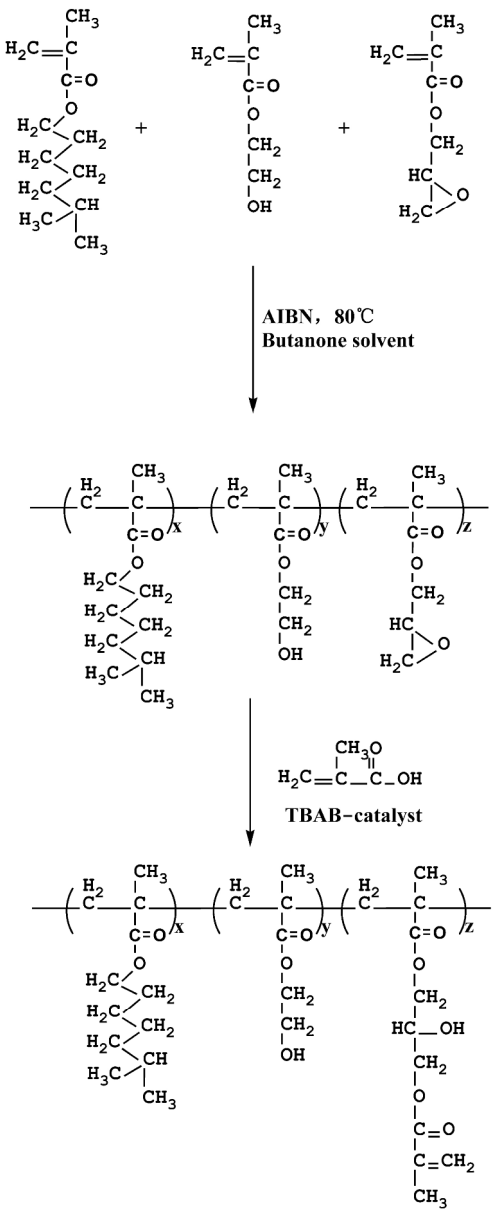

Scheme 1. Synthesis route of UV-cured PA
70x173mm (600 x 600 DPI)

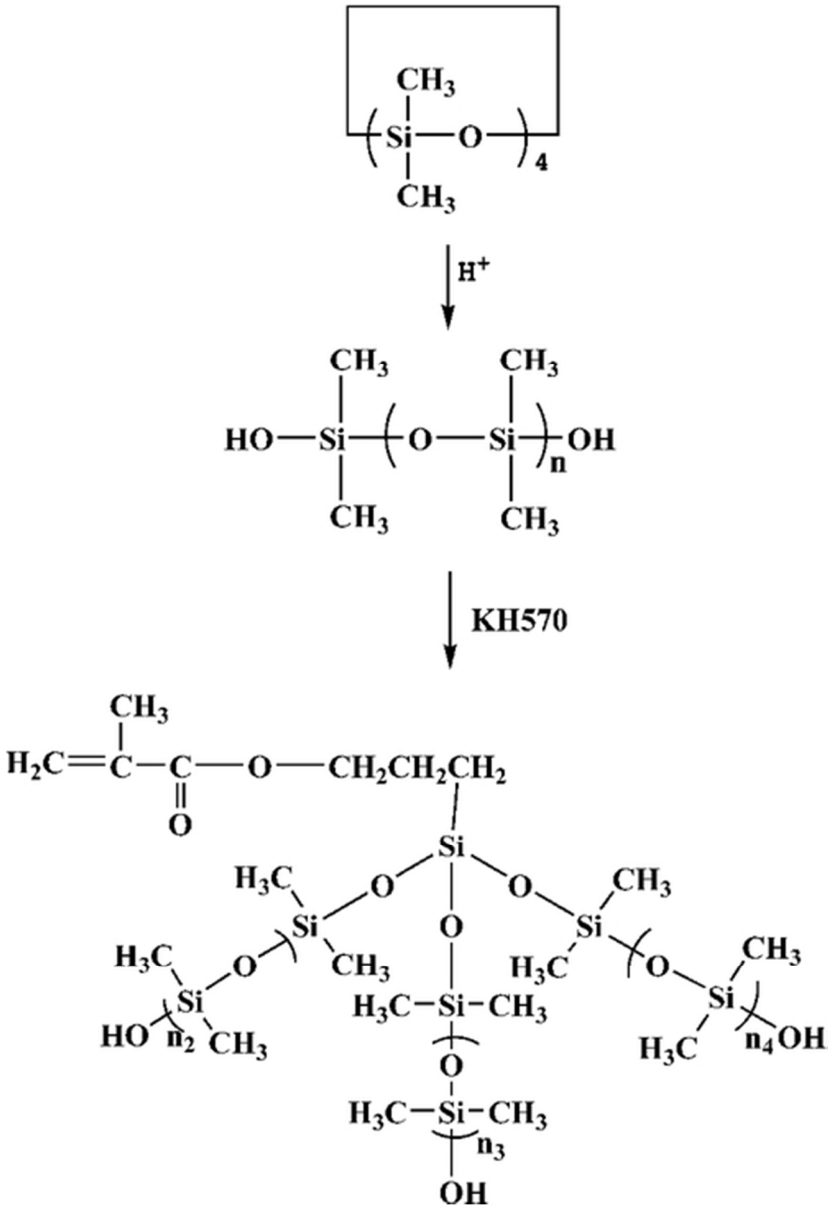

Scheme 2. Synthesis route of MATSi
21x30mm (600 x 600 DPI)

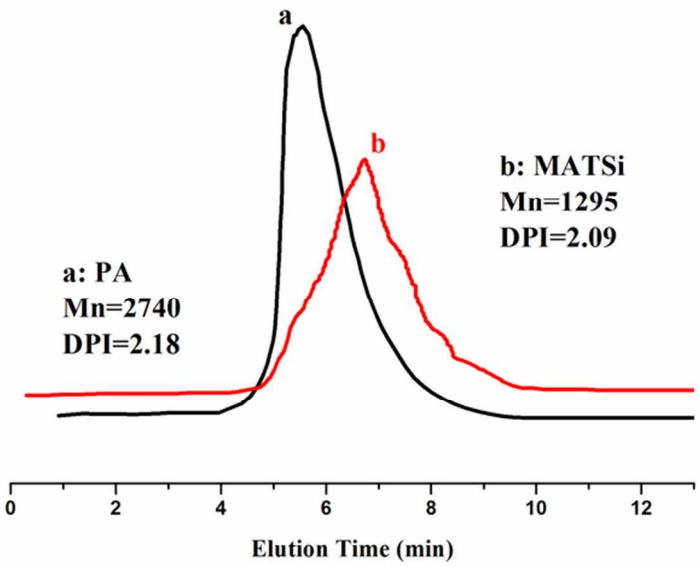

Fig.1. GPC traces of PA (a) and MATSi (b)
70x49mm (300 x 300 DPI)

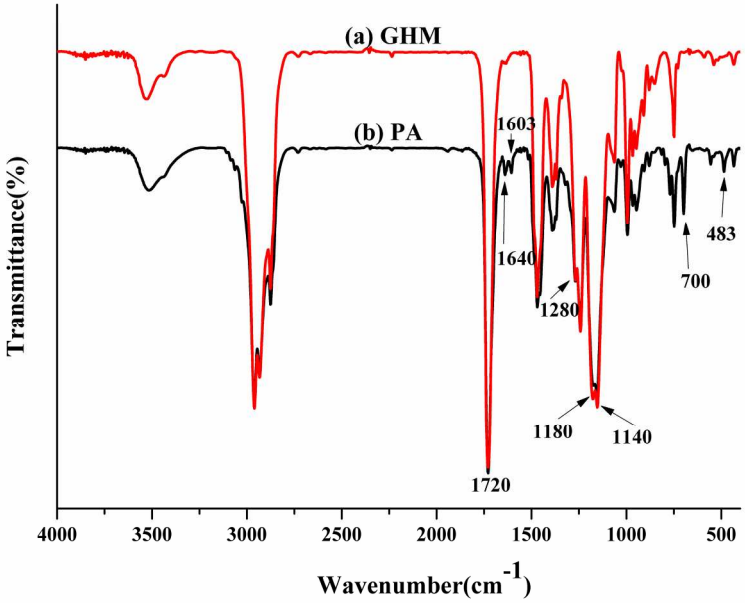

Fig.2. FT-IR spectra of GHM and PA
201x141mm (300 x 300 DPI)

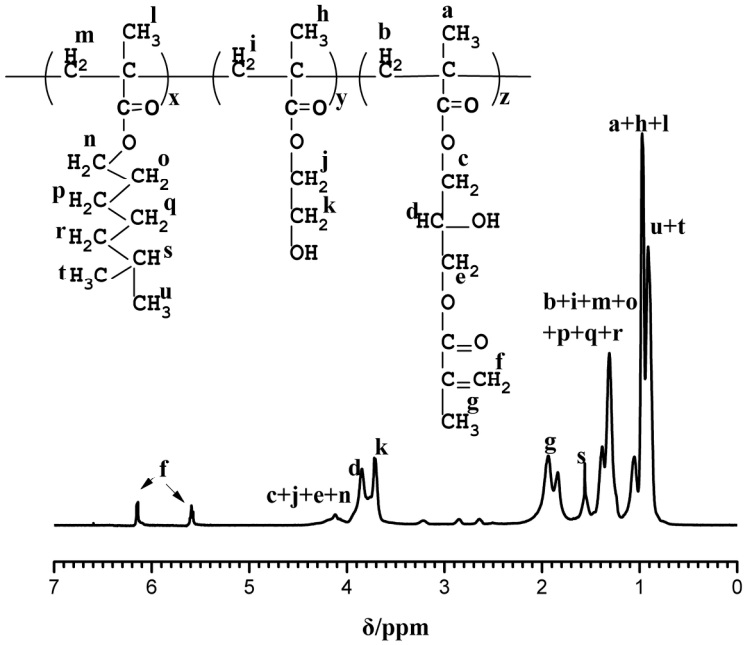

Fig.3. <1>H NMR spectra of PA
201x140mm (300 x 300 DPI)

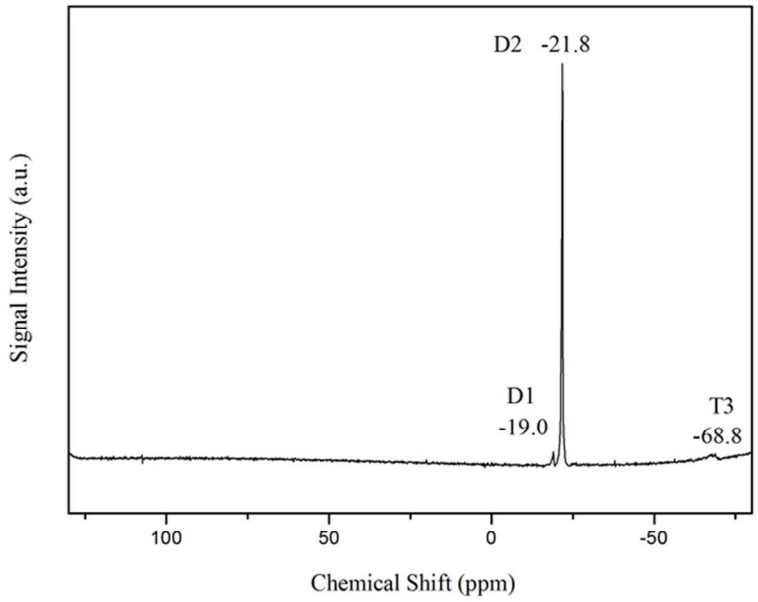

Fig.4. <29>Si NMR spectra of the synthesis of MATSi
70x49mm (300 x 300 DPI)

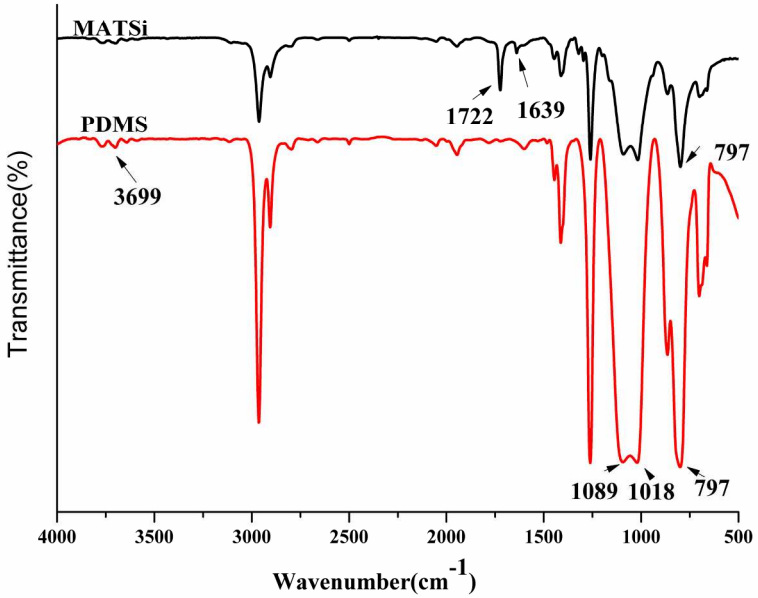

Fig.5. FT-IR spectra of the synthesis of MATSi
210x148mm (300 x 300 DPI)

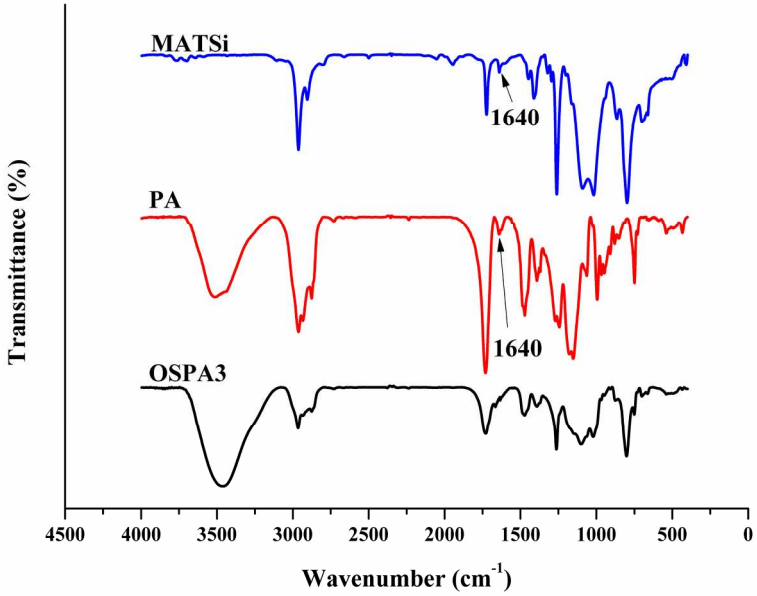

Fig.6. FT-IR spectra of the synthesis of OSPA
201x141mm (300 x 300 DPI)

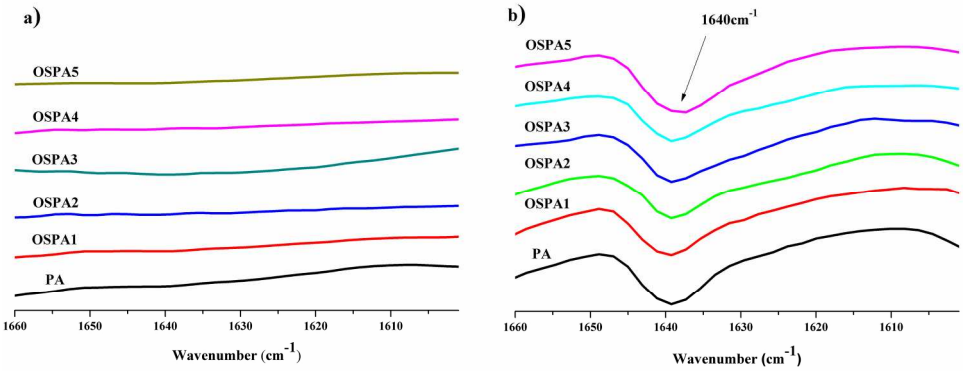

Fig.7. FT-IR spectra of the UV-curable film formulations of PA and OSPAs. a) Before irradiation; b) After UV-curing.
201x140mm (300 x 300 DPI)

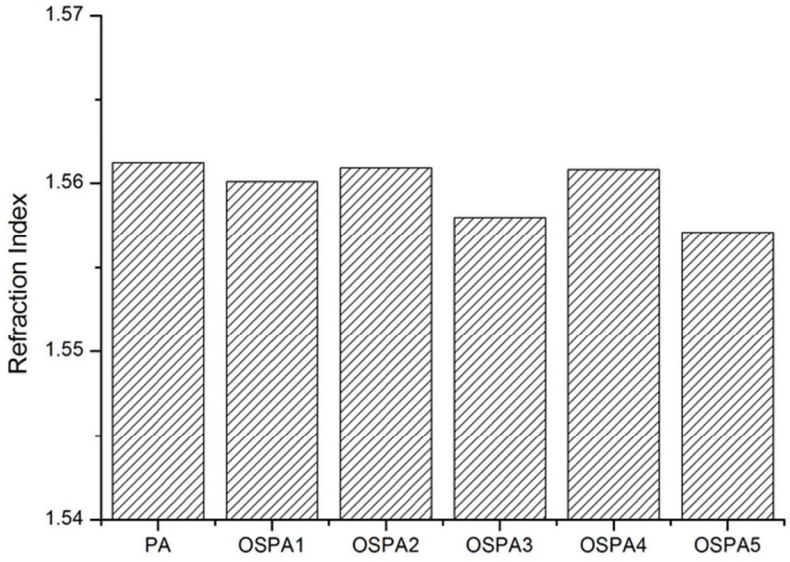

Fig.8. Refraction Indexes of the UV-cured coatings
70x49mm (300 x 300 DPI)

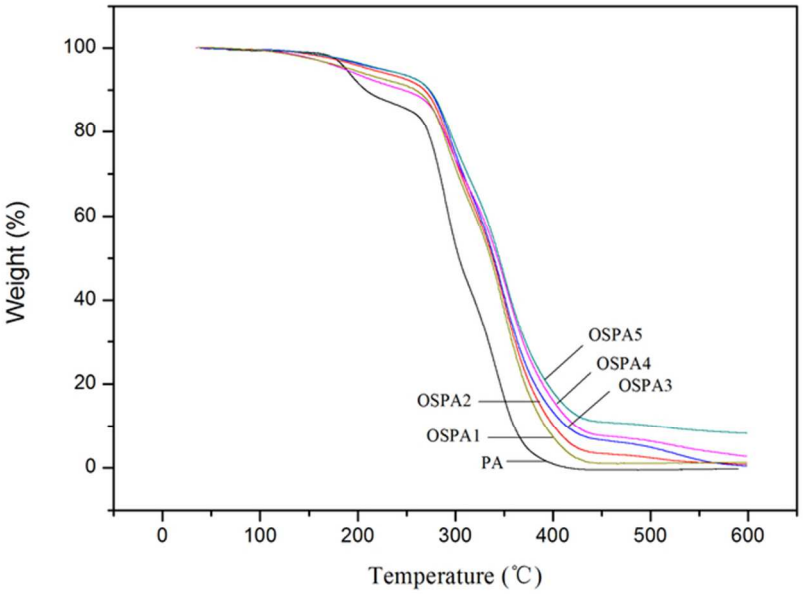

Fig.9. TGA curves of the UV-cured coatings
70x49mm (300 x 300 DPI)

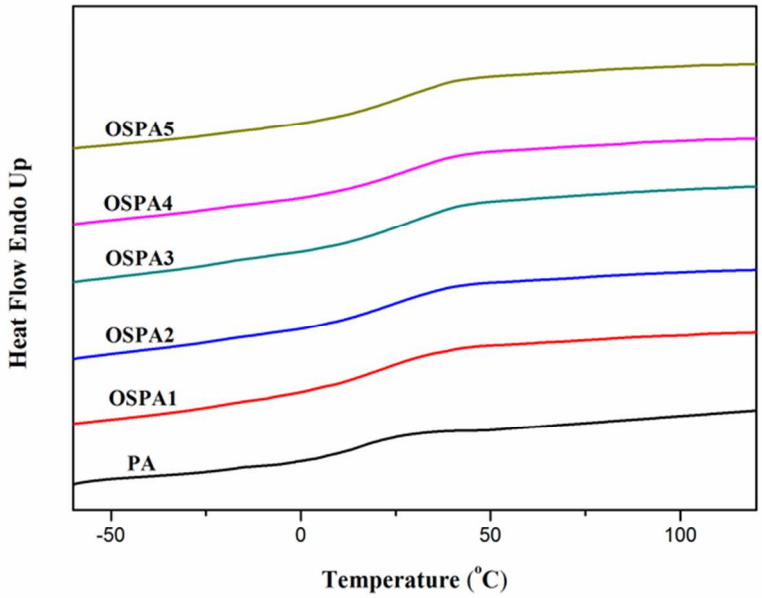

Fig.10. DSC thermograms of the UV-cured PA and OSPA coatings
70x49mm (300 x 300 DPI)

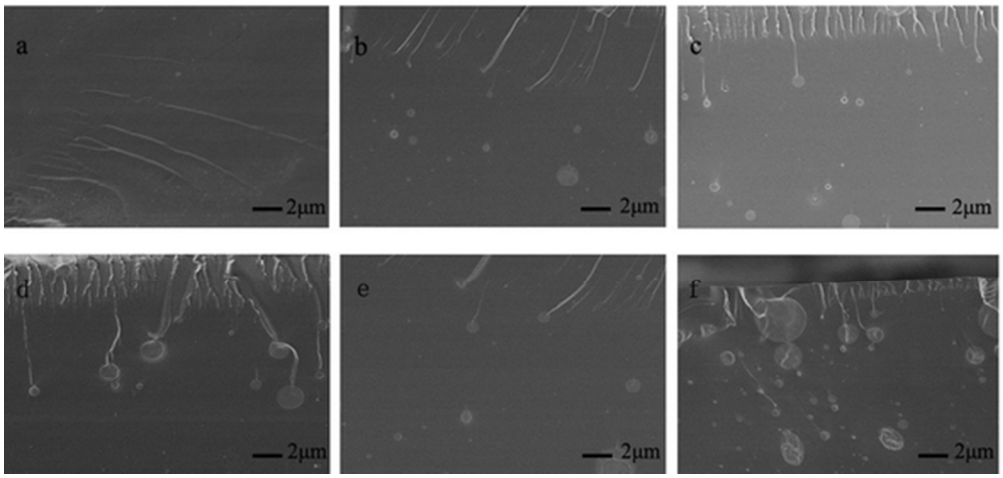

Fig.11. SEM images of fractured-surface morphologies of the UV-cured coatings: (a)PA; (b)OSPA1; (c)OSPA2; (d)OSPA3; (e)OSPA4; (f)OSPA5
49x23mm (300 x 300 DPI)

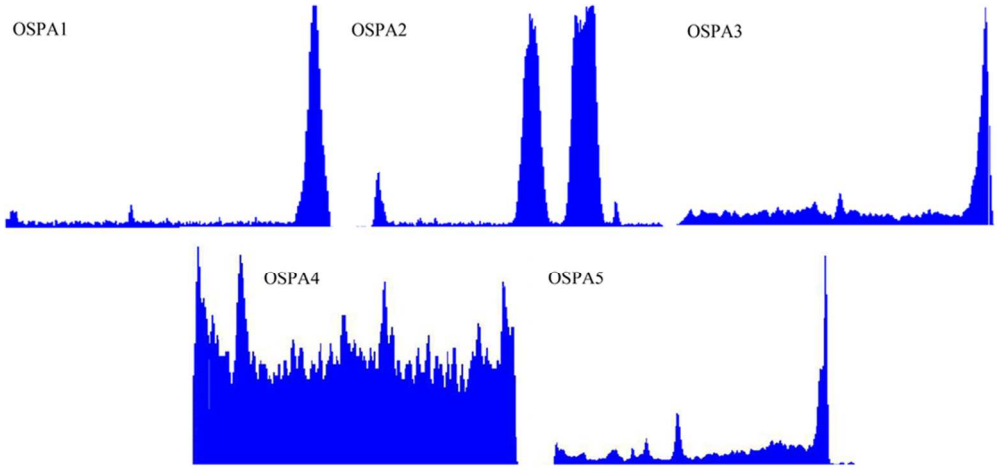

Fig.12. EDS images of fractured surface of the UV-cured coatings
90x90mm (300 x 300 DPI)

Table 1. Mass ratio of PA and MATSi.

Samples	PA (%)	MATSi (%)
Pure PA	100	0
OSPA1	98	2
OSPA2	96	4
OSPA3	94	6
OSPA4	92	8
OSPA5	90	10

Table 2. Molecular weights of PA and MATSi oligomers

Samples	Mn[a]	PDI[b]
PA	2740	2.18
MATSi	1295	2.09

[a] Mn: the number-average molecular weight, determined by GPC.

[b]PDI:the polydispersity index, determined by GPC.

Table 3. Degree of conversion of double bonds in the UV cured coatings

Coating	Conversion (%)
PA	95
OSPA1	96
OSPA2	97
OSPA3	99
OSPA4	97
OSPA5	98

Table 4.Gel content, flexibility and hardness characterization of the UV-cured coatings.

Samples	Gel content (%)	Flexibility			Pencil hardness
		8mm	6mm	5mm	
Pure PA	97	Fail	Fail	Fail	3H
OSPA1	98	Pass	Pass	Fail	5H
OSPA2	97	Pass	Pass	Pass	6H
OSPA3	98	Pass	Pass	Pass	6H
OSPA4	98	Pass	Pass	Pass	6H
OSPA5	98	Pass	Pass	Pass	6H

Table 5. Contact angle of the UV-cured coatings.

	Surface free energy(mN/m)	**Contact angle (θ°)with**	
	γ_s	Deionized water	Ethylene glycol
PA	44.28	94	55.75
OSPA1	11.70	102.5	91
OSPA2	12.73	108.5	91
OSPA3	10.36	108.5	94.5
OSPA4	13.27	109.5	91
OSPA5	8.89	114	99.5

γ_s surface free energy of solid.

Table 6. Thermal properties of the UV-cured coatings.

Sample	$T_{5\%}$	$T_{50\%}$	wt% at 600℃	T_g
PA	187.8	304.1	0	15.67
OSPA1	220.6	339.7	0.3	22.05
OSPA2	211.5	338.2	0.9	24.01
OSPA3	190.8	335.9	1.2	27.92
OSPA4	183.9	343.5	2.7	27.99
OSPA5	224.1	345.1	8.2	27.05